RM No. E7L10

NACA

RESEARCH MEMORANDUM

PERFORMANCE OF 24-INCH SUPERSONIC AXIAL-FLOW COMPRESSOR IN AIR

I - PERFORMANCE OF COMPRESSOR ROTOR AT DESIGN TIP SPEED OF 1600 FEET PER SECOND

By William K. Ritter and Irving A. Johnsen

Flight Propulsion Research Laboratory
Cleveland, Ohio

NATIONAL ADVISORY COMMITTEE
FOR AERONAUTICS

WASHINGTON
May 17, 1948

NATIONAL ADVISORY COMMITTEE FOR AERONAUTICS

RESEARCH MEMORANDUM

PERFORMANCE OF 24-INCH SUPERSONIC AXIAL-FLOW COMPRESSOR IN AIR

I - PERFORMANCE OF COMPRESSOR ROTOR AT DESIGN TIP SPEED OF 1600 FEET PER SECOND

By William K. Ritter and Irving A. Johnsen

SUMMARY

An axial-flow compressor rotor operating with supersonic velocities relative to the blade rows has been investigated in air at the NACA Cleveland laboratory to determine performance characteristics in air and to confirm the performance obtained in Freon-12 at the NACA Langley laboratory. The 24-inch-diameter rotor is aerodynamically similar to the Langley rotor, having very thin blades and a blade-tip shroud, but the structural design was refined to permit design operation at an actual tip speed of 1600 feet per second. The rotor was machined from a solid steel forging with the shroud integral with the blading. The performance of the rotor was experimentally obtained in a variable-component compressor that was designed and constructed for full-scale supersonic-compressor research over a wide range of air conditions. The rotor, installed without inlet guide vanes, was operated at an actual tip speed of 1634 feet per second, corresponding to an equivalent tip speed of 1608 feet per second.

A pressure ratio of 1.93 was obtained at an adiabatic efficiency of 0.79 and an equivalent weight flow of 58.12 pounds per second. This pressure ratio was somewhat higher than that obtained in the Freon-12 investigation at the same compressor Mach number with inlet guide vanes.

INTRODUCTION

A program of research on axial-flow compressors operating with supersonic velocities relative to the blade rows is being conducted by the NACA.

The first part of this investigation, including supersonic diffuser and cascade studies and the operation of an experimental compressor in Freon-12, was carried out at the NACA Langley laboratory. Reference 1 shows that supersonic diffusers can be designed to decelerate air from Mach numbers up to 2 through the speed of sound with efficiencies comparable to those obtained in good subsonic diffusers. Theoretical results presented in reference 2 indicated that confining the normal shock within cascade blading eliminates the extended wave system that usually is responsible for the large losses in the supersonic flow about isolated bodies. An experimental supersonic compressor was therefore designed on the basis of these preliminary studies and was operated at low pressure in Freon-12 at the Langley laboratory (reference 3). Freon-12 (dichlorodifluoromethane (CCl_2F_2), a commercial refrigerant) was used as the testing medium because its sonic velocity is approximately one-half that of air and an experimental rotor could thus be constructed without the difficulty of providing the high structural efficiency required for operation in air.

A variable-component supersonic compressor has been designed and constructed at the NACA Cleveland laboratory for full-scale supersonic-compressor research over a wide range of altitude air conditions. Initial steps in this program were to achieve full-speed operation of a supersonic compressor in air and to confirm, in air, the performance obtained in Freon-12. The rotor used is aerodynamically similar to the rotor of reference 3, having very thin blades and a blade-tip shroud, but the structural design was refined for design operation at an actual tip speed of 1600 feet per second. The invaluable assistance of S. S. Manson of the Stress and Vibration Section of the Cleveland laboratory in the structural design of the rotor is gratefully acknowledged.

Because of the high centrifugal stresses and the danger of destructive vibration in the thin blades of this supersonic-compressor rotor, experimental investigations were made of blade vibrations in cascades and on the rotor during operation. Results of the vibration investigation, conducted by the Stress and Vibration Section, will be reported separately.

The supersonic-compressor rotor is described and the performance results for the compressor operating without inlet guide vanes at approximately the design equivalent tip speed of 1600 feet per second are given.

COMPRESSOR ROTOR

The supersonic-compressor rotor designed and constructed for this investigation is shown in figure 1. Structural strength, accuracy of dimensions, and freedom from operating distortions were primary considerations in this rotor design. The 62 blades are substantially the same as those of the supersonic-compressor rotor of reference 3, the differences being that the blade-tip diameter was 24 instead of 16 inches, the blade form was developed in cylindrical coordinates for closer conformity with assumed air flow, and the proportional thickness of the blades was increased to reduce severity of blade vibrations.

Mechanical design of rotor. - Because very thin blades were used in this rotor, the blades had to be supported at the tips to prevent destructive vibration. The rotor was made in one piece rather than start a development program of indefinite duration to provide a method of attaching a rim or shroud to the blades that could operate at the design speed of 1600 feet per second. The shroud had to be restrained by the blades, of course, to reduce the stress in the shroud. Steel blades were desired so that the sharp edges would have good resistance to buffeting; the rotor was therefore machined from a solid steel forging. An alloy steel was used having good deep-hardening characteristics and a tensile yield strength of about 135,000 pounds per square inch.

The design stresses of this supersonic-compressor rotor at a tip speed of 1600 feet per second were: disk stress, about 50,000 pounds per square inch; blade steady stress, 85,000 pounds per square inch; and a shroud stress somewhat higher than the blade stress. The cross section of the shroud was proportioned for stiffness and light weight. Fillets of 0.125-inch radius were used at the blade roots and at the blade tips. The fillets were faired into the sharp edges of the blades.

Rotor blading. - The rotor form and the dimensions of a normal blade section at the pitch radius are shown in figure 2. These blades were designed to operate (with inlet guide vanes) at a compressor Mach number of 1.43, which corresponds to an equivalent tip speed of approximately 1600 feet per second. The blades have a constant chord from hub to tip, sufficient blade twist to maintain radial elements, and no radial taper in thickness. Blade entrance angles, discharge angles, geometrical turning angles, and leading- and trailing-edge wedge angles for the root, pitch, and tip sections are given in the following table:

Location	Entrance angle (deg)	Discharge angle (deg)	Turning angle (deg)	Wedge angle (deg)
Root (9.00-in. rad)	33.28	43.22	9.93	10.00
Pitch (10.50-in. rad)	29.83	38.47	8.63	10.00
Tip (12.00-in. rad)	27.07	34.42	7.35	10.00

A preliminary investigation of the vibration characteristics of the blades indicated that blades thicker than the original design would probably be required. The application of a method for determining the limiting contraction ratio for supersonic-compressor blading (reference 4) indicated that a blade having 50 percent greater minimum thickness could satisfy the aerodynamic requirements of this compressor. A five-blade rectangular cascade of supersonic blades having the form and spacing of the blade-root section (most critical aerodynamically) and having blades integral with the root and tip supports was installed in an open-jet supersonic wind tunnel, and aerodynamic and vibratory characteristics were investigated simultaneously (reference 4). As a result of this investigation, the minimum blade thickness of the original design was increased by 50 percent, to the values shown in figure 2. Data obtained indicated that this increase in blade thickness reduced the vibratory stress to an acceptable level and that shock would enter the blading at the design Mach number provided that the wedge angle at the leading edge of the blade was less than that required for the attachment of shock.

APPARATUS

Variable-Component Compressor

A photograph of the variable-component-compressor installation is shown in figure 3; a diagrammatic cross section of the unit is shown in figure 4. Air, which is inducted directly from the test cell, passes through a measuring orifice located in the inlet pipe. An electrostatic air filter is provided to filter all dust and particles from the air before it reaches the rotor. A depression tank, 6 feet in diameter and 10 feet in length, is located ahead of the compressor to insure smooth entry of the air, in accordance with the standard procedures for axial-flow compressors (reference 5).

A wood inlet section accelerates the air from a Mach number of less than 0.1 (at design flow) to the inlet axial Mach number of

approximately 0.8. The characteristics of the inlet-section fairings, which were designed on the basis of potential-flow theory, were investigated in a half-scale mockup. These studies showed that a flat axial-velocity profile existed across 99.6 percent of the half-scale passage at the rotor-entrance station with a displacement boundary layer of 0.0025 inch on each wall. The installation contains a removable spacer to permit shifting of the inlet section and thus to provide space for the future installation of guide vanes ahead of the rotor.

The rotor has a cantilever mounting arrangement, with the shaft supported on three self-alining journal bearings. Aluminum air-seal rings are located at rotor root and tip to provide minimum axial clearance and thereby prevent excessive leakage through the clearance gap. A straight annular passage is provided behind the rotor for instrumentation and for future installation of stator blading.

Air discharges into the variable-component collector through a constant-area radial-flow diffuser section. The air is discharged from the collector through two radial outlet pipes to a common line connected to the laboratory altitude-exhaust facilities.

Compressor pressures are regulated by butterfly throttle valves located in the inlet and outlet pipes. The compressor is driven by a 9000-horsepower variable-frequency induction motor through a speed-increaser gear to provide a maximum speed of about 16,000 rpm.

Instrumentation

The air weight flow through the compressor was measured by a 20-inch-diameter adjustable orifice located in a straight section of the inlet piping. The pressure drop across the orifice was measured by a water manometer; the upstream pressure was measured by a mercury manometer. Two thermocouples and two total-pressure tubes immediately upstream of the orifice were used to measure the state of the air entering the orifice.

Measurements at the inlet to the compressor were made in the depression tank, as recommended in reference 5. Two thermocouple rakes, located 180° apart, were installed; each rake consisted of three thermocouples located at the area centers of equal annular areas. A calibration check verified the fact that the velocity of the air was negligible in the tank and that the two static-pressure taps, installed as recommended in reference 5, could be used to measure total pressure.

Measurements downstream of the rotor were made by means of a calibrated survey instrument located approximately $1\frac{1}{2}$ inches downstream of the rotor. The survey instrument consisted of a "null" type yaw meter, a static-pressure tube and a total-pressure tube (fig. 5) and was used to measure direction of flow, static pressure, and total pressure of the air, respectively. The static-pressure tube was calibrated over the range of Mach numbers encountered in operation. The biggest source of error in the survey measurements is the static pressure as given by the static-pressure tube. Experimental data indicate that under certain operating conditions, the static pressures as measured by the survey tube do not check the corresponding wall tap readings at the same axial station. The discrepancy can be attributed to the calibration of the static-pressure tube in an undisturbed air stream, whereas the actual air stream at the rotor outlet probably has turbulence and radial-flow components. Total-pressure and angle measurements are believed to be smaller sources of error than the static pressures. The survey instrument was mounted in a remotely operated motor-driven survey mechanism that provided separate control of rotation and translation of the tube (fig. 5).

Two thermocouple rakes and two total-pressure rakes, spaced 180° apart, were located approximately $13\frac{1}{2}$ inches downstream of the rotor. Each rake consisted of three instruments located at the area centers of equal annular areas. The tubes were found to be insensitive to yaw over a range of approximately $\pm 30^\circ$; at each speed, the rakes could therefore be set to give accurate readings over the range of air flows and air-discharge angles encountered. Each tube of the thermocouple rake was calibrated for recovery coefficient over the Mach number range of the investigation.

The compressor-inlet section was extensively instrumented with static-pressure taps along the entire flow length and on both inner and outer wall surfaces. Four static-pressure taps, spaced 90° apart, were provided on both the inner and outer walls at the survey station $1\frac{1}{2}$ inches downstream of the rotor. Two static-pressure taps, spaced 180° apart, were located on each wall at the rake station $13\frac{1}{2}$ inches downstream of the rotor.

All pressures were measured with mercury manometers and all temperatures were taken with calibrated iron-constantan thermocouples. The difference in potential between the hot junction and the ice bath was measured with a sensitive calibrated potentiometer

in conjunction with a spotlight galvanometer. The speed of the rotor was measured with an electric chronometric tachometer.

Strain gages were installed on the rotor blading at the point of maximum stress, as indicated in the blade-cascade investigation, for measuring vibratory stresses in operation.

PROCEDURE

The compressor was investigated at approximately the design equivalent tip speed of 1600 feet per second with inlet air inducted from the test cell at a temperature of approximately 77° F. The actual tip speed was 1634 feet per second, and the operating equivalent tip speed was 1608 feet per second, corresponding to a compressor Mach number of 1.44.

An extensive investigation was made of the vibratory characteristics of the blades over a large range of angle of attack and rotational speed before the operation of the compressor at design speed. In the subsonic regime of operation, the minimum vibratory stress was found to occur near an angle of attack of 0° and vibratory stresses increased with increasing angle of attack, both positive and negative. With increasing rotational speed, however, the range of angle of attack over which the compressor operated was reduced. As a consequence, the entire subsonic range of operation could be covered without serious vibratory stress.

In the supersonic range of operation, the aerodynamic characteristics of the rotor limited the flow to angles of attack near 0°. As a result, the vibratory stresses were small in normal operation at the high speeds. A minimum back pressure was maintained while the speed was increased in the supersonic range; shock was thus allowed to enter the rotor. The various operating points were then set by increasing the back pressure and thereby forcing the shock wave upstream in the rotor. Air flow was varied from wide-open throttle to stall.

At each point, a complete set of pressure and temperature readings was obtained and a 12-station survey of pressure and flow angle was made across the passage behind the rotor. Sufficient time was taken in the survey to allow for stabilization of the flow and for the inherent lag in the long pressure-tube connections. From survey data, the axial and tangential velocities, the Mach numbers, the pressures, and the densities may be determined.

The following measures of performance were used (all symbols are defined in appendix A and a detailed description of the methods of computation is given in appendix B.):

1. Weight flow W, pounds per second

   (a) Integrated weight flow based on measurements made at survey station

   (b) Weight flow measured by means of 20-inch adjustable orifice

2. Useful work of compression H_{ad}, foot-pound per pound mass

   (a) Weight-flow average of useful work of compression, $H_{ad,W}$ based on total pressures measured at the survey station

   (b) Area average of useful work of compression, based on arithmetic average of total pressures measured at area centers of three equal annular areas at rake station, $H_{ad,A}$

3. Total work of compression H, foot-pounds per pound mass

   (a) Weight-flow average of total work of compression based on rotational velocity given to air, measured at the survey station, H_W

   (b) Area average of total work of compression based on arithmetic average of total temperatures measured at area centers of three equal annular areas at rake station, H_A

4. Total-pressure ratio P/P_1

   (a) Weight-flow average of total-pressure ratio based on total pressures measured at survey station, $(P_5/P_1)_W$

   (b) Area average of total-pressure ratio based on arithmetic average of total pressures measured at area centers of three equal annular areas at rake station, $(P_6/P_1)_A$

5. Adiabatic efficiency η_{ad}

(a) $\eta_{ad,W} = H_{ad,W}/H_W$

(b) $\eta_{ad,A} = H_{ad,A}/H_A$

(c) $\eta_{ad,T} = H_{ad,W}/H_A$

RESULTS AND DISCUSSION

Weight flow. - As shown in the following table, the weight flows obtained by an integration across the rotor passage at the survey station checked the orifice weight flows to within 3 percent:

Equivalent weight flow $W\sqrt{\theta}/\delta$ (lb/sec)	Orifice weight flow, W (lb/sec)	Integrated weight flow, W (lb/sec)	Discrepancy (percent)
58.12	29.15	29.97	2.8
60.28	26.63	27.04	1.5
61.25	26.66	26.26	1.5
62.26	28.43	29.24	2.8

Inasmuch as the variation is of the order of the accuracy of the adjustable orifice, the survey data are considered satisfactory.

Work of compression. - The values of H_{ad} and H, the useful and total work of compression, respectively, are shown in figure 6 as a function of equivalent weight flow $W\sqrt{\theta}/\delta$ for the operating equivalent tip speed of 1608 feet per second. The weight-flow averages of the useful work of compression $H_{ad,W}$ based on total pressures measured in the survey downstream of the rotor are consistently higher than the area average $H_{ad,A}$ obtained by using the downstream-rake total pressures. This difference may be attributed to the effect of the weight-flow averaging, for the highest velocities and total pressures occurred near the pitch section, and to a drop in total pressure from the survey station to the rake station. The variation in total-pressure ratio and weight flow per increment of radius across the passage is shown in figure 7 for a typical operating condition.

The values for total work of compression based on the rotation imparted to the air H_W showed reasonably good agreement with those obtained from an arithmetic average of total temperatures measured by the downstream rakes H_A (fig. 6). The maximum discrepancy between H_A and H_W was of the order of $1\frac{1}{2}$ percent.

Pressure ratio and adiabatic efficiency. - The pressure ratio and the adiabatic efficiency of the supersonic-compressor rotor are shown as functions of equivalent weight flow at the equivalent tip speed of 1608 feet per second in figure 8. The pressure ratio shows the same trend as the useful work of compression (fig. 6); the weight-flow average at the survey station $(P_5/P_1)_W$ is higher than the area average at the rake station $(P_6/P_1)_A$ A peak pressure ratio of 1.93 was obtained at the survey station with an equivalent weight flow of 58.12 pounds per second. This pressure ratio is somewhat higher than the peak pressure ratio of 1.84 that was obtained in the Langley Freon experiments at the same compressor Mach number with inlet guide vanes (reference 3).

The adiabatic-efficiency curves of figure 8 show close agreement between $\eta_{ad,W}$ and $\eta_{ad,T}$, for the useful work of compression is based on the pressure survey directly behind the rotor in each case. A peak value of $\eta_{ad,T}$ of approximately 0.79 was obtained. This peak efficiency occurred at the peak-pressure-ratio point, in accordance with the results of reference 3 and supersonic theory.

The values of $\eta_{ad,A}$ based on the pressures measured at the downstream rake are consistently lower than the values of $\eta_{ad,T}$ and $\eta_{ad,W}$ and show a peak efficiency of approximately 0.78. The data indicate that this decrease in efficiency is the result of weight-flow averaging and of small losses in total pressure from the survey station to the rake station. Although the values of $\eta_{ad,T}$ are indicative of the performance evaluated at the rotor discharge, the values of $\eta_{ad,A}$ give a more representative evaluation of the efficiency at which the compressor operates, for they include some of the losses associated with the equalization of the nonuniform total-energy gradient across the rotor passage.

Entry of shock. - In the construction of the compressor, the rotor was machined to maintain the 10° wedge at the leading edge of the blade, as in the Langley rotor. Operating the

compressor without inlet guide vanes at a tip speed of 1608 feet per second, however, resulted in an inlet relative Mach number in the region near the hub that theoretically was lower than that required for the attachment of a shock wave to a 10° wedge. Therefore shock probably did not enter the rotor in the region near the hub and true supersonic flow did not exist over the entire rotor entrance at the design speed. The weight-flow characteristic of figure 8 indicates that this condition was true, because with supersonic operating conditions across the entire annulus, no variation in weight flow should occur with a change in back pressure. Supersonic conditions across the entire rotor can probably be attained by reducing the wedge angle, by increasing the Mach number at the hub by the use of inlet guide vanes, or by running at a higher compressor Mach number.

SUMMARY OF RESULTS

An investigation of the performance of a 24-inch axial-flow supersonic-compressor rotor having very thin blades and a shroud at the blade tip, in air in a variable-component compressor, gave the following results:

1. The supersonic-compressor rotor could be operated at an actual tip speed of 1634 feet per second.

2. At an equivalent tip speed of 1608 feet per second, a pressure ratio of 1.93 was obtained at an adiabatic efficiency of 0.79 and an equivalent weight flow of 58.12 pounds per second.

Flight Propulsion Research Laboratory,
National Advisory Committee for Aeronautics,
Cleveland, Ohio.

APPENDIX A

SYMBOLS

The following symbols are used in the determination of compressor performance:

a	local velocity of sound, ft/sec
c_p	specific heat of normal air at constant pressure, 0.243 Btu/(lb)($^\circ$F)
g	acceleration due to gravity, 32.174 ft/sec^2
H	total work of compression, increase in total enthalpy per unit mass, ft-lb/lb mass
H_{ad}	useful work of compression, isentropic increase in total enthalpy for given pressure rise, ft-lb/lb mass
J	mechanical equivalent of heat, 778 ft-lb/Btu
M	Mach number, ratio of velocity to local velocity of sound (V/a)
n	rotor speed, rps
P	total or stagnation pressure, lb/sq ft absolute
p	static or stream pressure, lb/sq ft absolute
R	gas constant for normal air, 53.50 ft-lb/(lb)($^\circ$F)
r	compressor radius, ft
T	total or stagnation temperature, $^\circ$R
t	static or stream temperature, $^\circ$R
U	velocity of rotor ($2\pi rn$) at radius r, ft/sec
V	absolute air velocity, ft/sec
W	weight flow, lb/sec

β angle between compressor axis and absolute air velocity, degrees

γ ratio of specific heats for normal air, 1.400

δ ratio of actual inlet total pressure to standard sea-level pressure ($P_1/2116$)

η_{ad} adiabatic efficiency

θ ratio of actual inlet stagnation temperature to standard sea-level temperature ($T_1/518.4$)

ρ density, lb/cu ft

The subscripts denote the following conditions:

1 compressor inlet

5 survey measuring station

6 rake measuring station

A area average

i inner radius

o outer radius

T temperature-rise basis

W weight-flow average

z axial component

APPENDIX B

PERFORMANCE-COMPUTATION METHODS

Weight flow. - The integrated discharge weight flow is computed from the measured data P_5, p_5, β_5, and T_6:

$$W = \int_{r_i}^{r_o} 2\pi r_5 \frac{p_5}{Rt_5} V_5 \cos \beta_5 \, dr_5 \qquad (1)$$

where

$$t_5 = T_5 \left(\frac{p_5}{P_5} \right)^{\frac{\gamma-1}{\gamma}}$$

and, by the assumption of no heat transfer from station 5 to station 6,

$$T_5 = T_6$$

and where

$$V_5 = M_5 a_5$$

or

$$V_5 = 49.04 \left\{ \frac{2t_5}{\gamma-1} \left[\left(\frac{P_5}{p_5} \right)^{\frac{\gamma-1}{\gamma}} - 1.0 \right] \right\}^{\frac{1}{2}}$$

The weight flow was obtained by graphical integration of equation (1). This integrated weight flow was checked against the weight flow measured by the adjustable orifice to obtain an indication of the accuracy of the survey data.

Useful work of compression. - A weight-flow average of the useful work of compression is obtained by a graphical integration using survey-station data:

$$H_{ad,W} = \frac{\int_{r_i}^{r_o} 2\pi r_5 \frac{p_5}{Rt_5} V_5 \cos \beta_5 \, c_p \, JT_1 \left[\left(\frac{P_5}{P_1}\right)^{\frac{\gamma-1}{\gamma}} - 1.0\right] dr_5}{W_5}$$

An area average of the useful work of compression at the rake station is obtained by using an arithmetic average of the total pressures at the area centers of three equal areas:

$$H_{ad,A} = c_p JT_1 \left[\left(\frac{P_6}{P_1}\right)^{\frac{\gamma-1}{\gamma}} - 1.0\right]$$

Total work of compression. - A weight-flow average of the total work of compression is obtained by a graphical integration of the work done in turning the air, measured at the survey station:

$$H_W = \frac{\int_{r_i}^{r_o} 2\pi r_5 \frac{p_5}{Rt_5} V_5 \cos \beta_5 \frac{UV_5 \sin \beta_5 \, dr_5}{g}}{W_5}$$

An area average of the total work of compression at the rake station is obtained by using an arithmetic average of the total temperatures measured at the area centers of the three equal areas.

$$H_A = c_p J (T_5 - T_1)$$

Total-pressure ratio. - A weight-flow average of the pressure ratio measured at the survey station behind the rotor is obtained from the integrated useful work of compression:

$$\left(\frac{P_5}{P_1}\right)_W = \left[\frac{H_{ad,W}}{c_p J T_1} + 1.0\right]^{\frac{\gamma}{\gamma-1}}$$

The area average of total-pressure ratio is simply the arithmetic average of the total pressures at the area centers of the three equal annular areas at the rake station divided by the total pressure at the inlet: $(P_6/P_1)_A$.

Adiabatic efficiency. - Several methods of determining η_{ad} using the various values of H_{ad} and H are available. A weight-flow-average adiabatic efficiency, measured at the survey station directly behind the rotor, is given by the following expression:

$$\eta_{ad,W} = \frac{H_{ad,W}}{H_W}$$

This efficiency term corresponds to that used in reference 3.

An area-average adiabatic efficiency, measured at the rake station downstream of the rotor, is calculated as

$$\eta_{ad,A} = \frac{H_{ad,A}}{H_A}$$

This efficiency is generally lower than $\eta_{ad,W}$ because of the decrease in the apparent useful work of compression from the survey station to the rake station.

The value of static pressure is critical in calculating the total work of compression based on rotational velocity given to the air H_W. The values of H_W are therefore somewhat inconsistent, since static pressure is the biggest source of error in the survey measurements. Experimental results over the greater portion of the operating range, however, indicate that the assumption of no heat transfer from the survey station to the rake station can be made with little error. Therefore, a more valid expression for the adiabatic efficiency directly behind the rotor can be given by

$$\eta_{ad,T} = \frac{H_{ad,W}}{H_A}$$

The $\eta_{ad,T}$ term corresponds to the adiabatic temperature-rise efficiency of reference 5, and appears to give the more consistent and accurate evaluation of the compressor efficiency at that station.

REFERENCES

1. Kantrowitz, Arthur, and Donaldson, Coleman du P.: Preliminary Investigation of Supersonic Diffusers. NACA ACR No. L5D20, 1945.

2. Kantrowitz, Arthur: The Supersonic Axial-Flow Compressor. NACA ACR No. L6D02, 1946.

3. Erwin, John R., Wright, Linwood C., and Kantrowitz, Arthur: Investigation of an Experimental Supersonic Axial-Flow Compressor. NACA RM No. L6J01b, 1946.

4. Wright, Linwood C.: Investigation to Determine Contraction Ratio for Supersonic-Compressor Rotor. NACA RM No. E7L23, 1948.

5. NACA Subcommittee on Compressors: Standard Procedures for Rating and Testing Multistage Axial-Flow Compressors. NACA TN No. 1138, 1946.

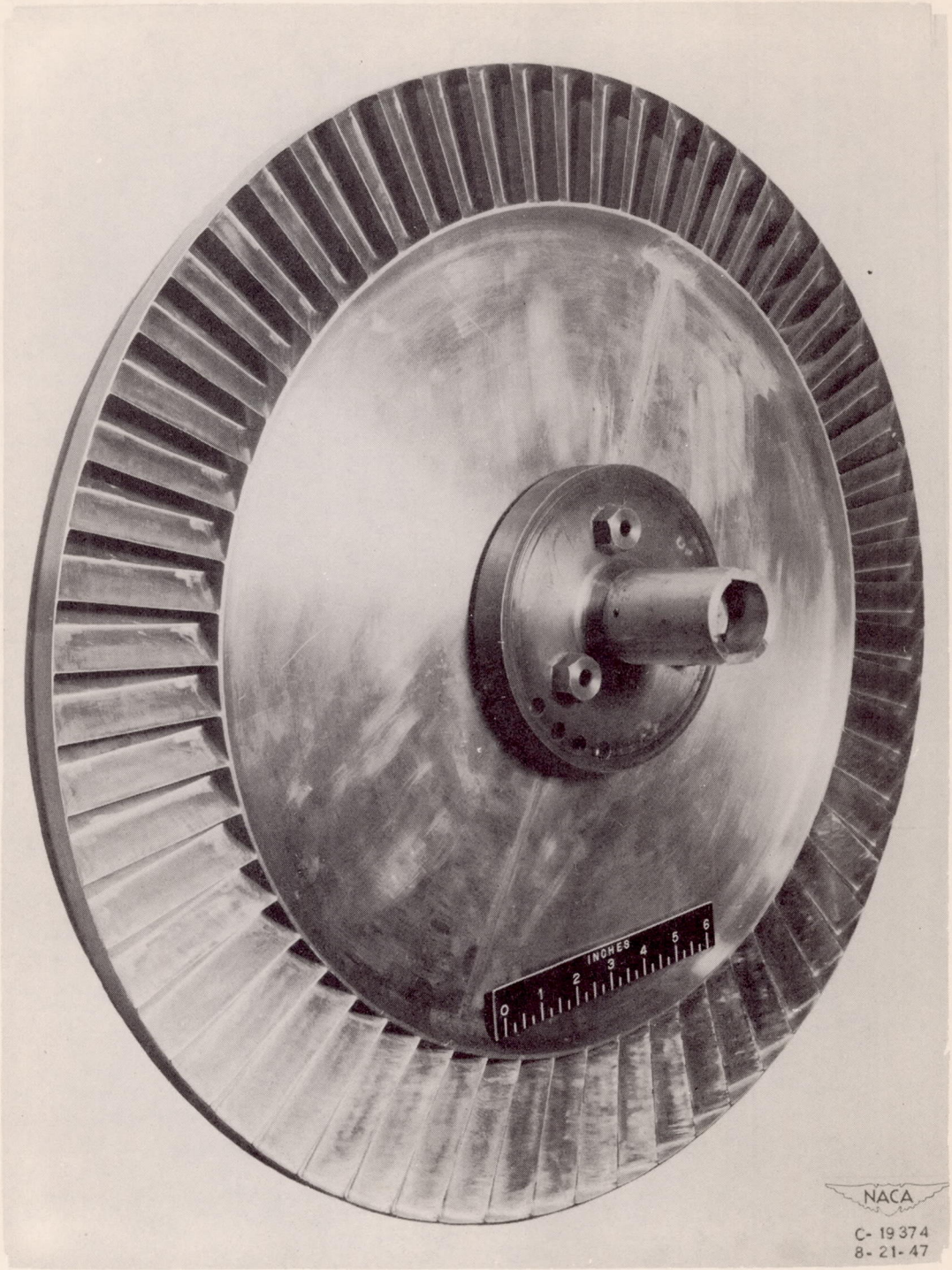

Figure 1. - The 24-inch supersonic-compressor rotor.

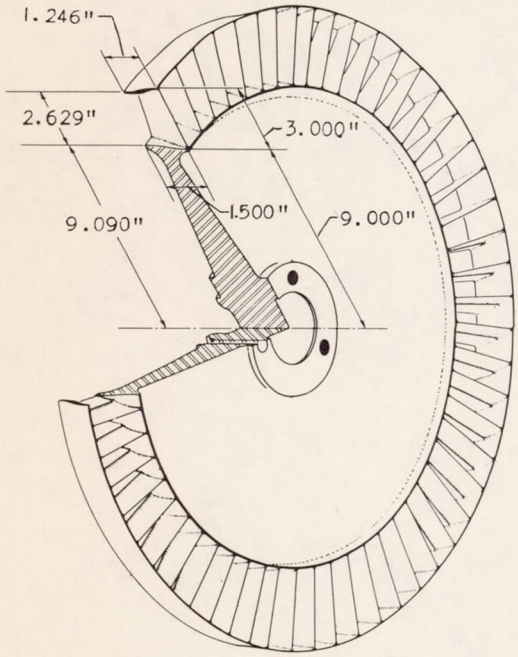

(a) Supersonic-compressor rotor.

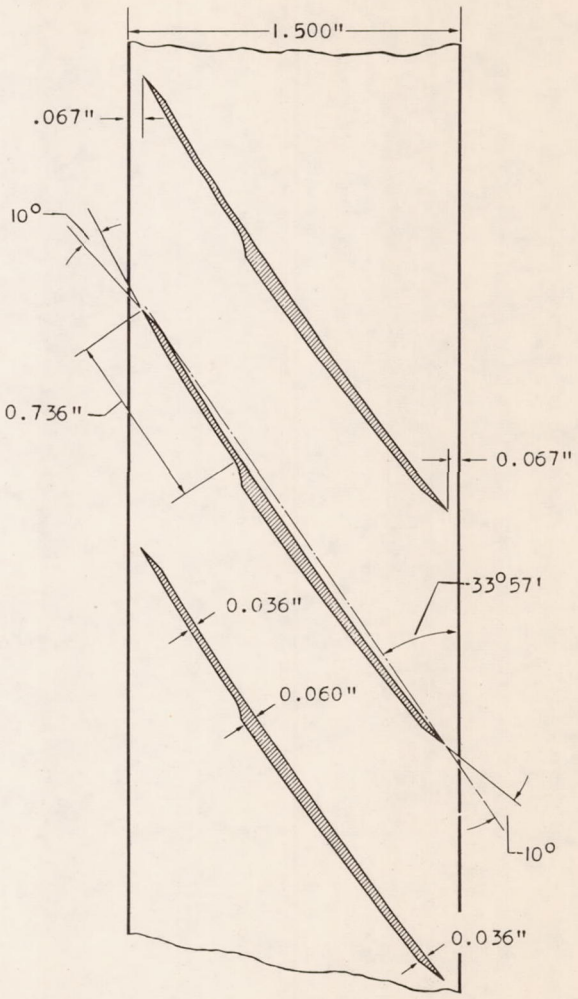

(b) Normal cross section through blades at pitch radius, 11.500 inches.

NACA

Figure 2. - Sectional view of 24-inch supersonic-compressor rotor and blades.

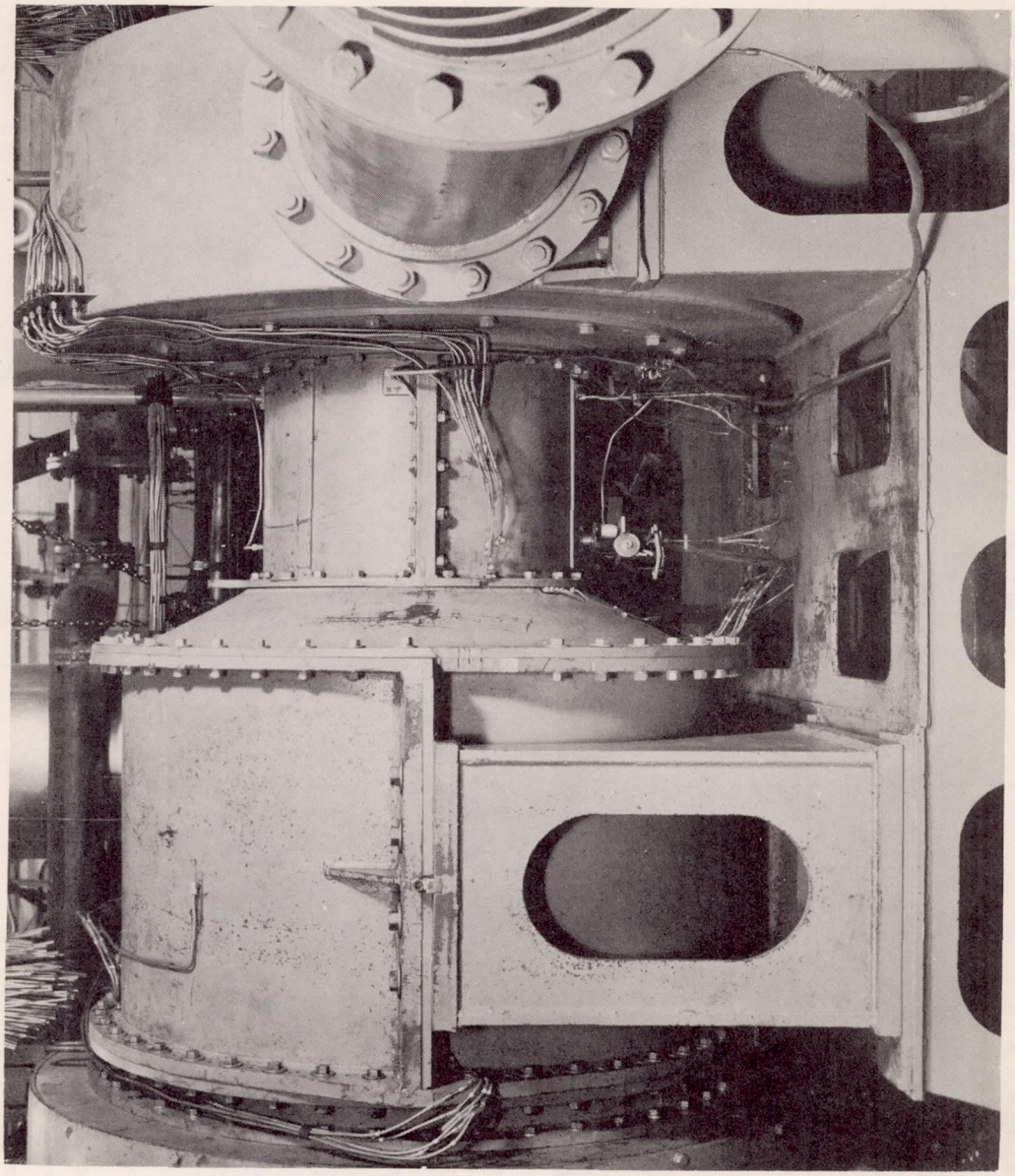

Figure 3. - Variable-component supersonic-compressor installation.

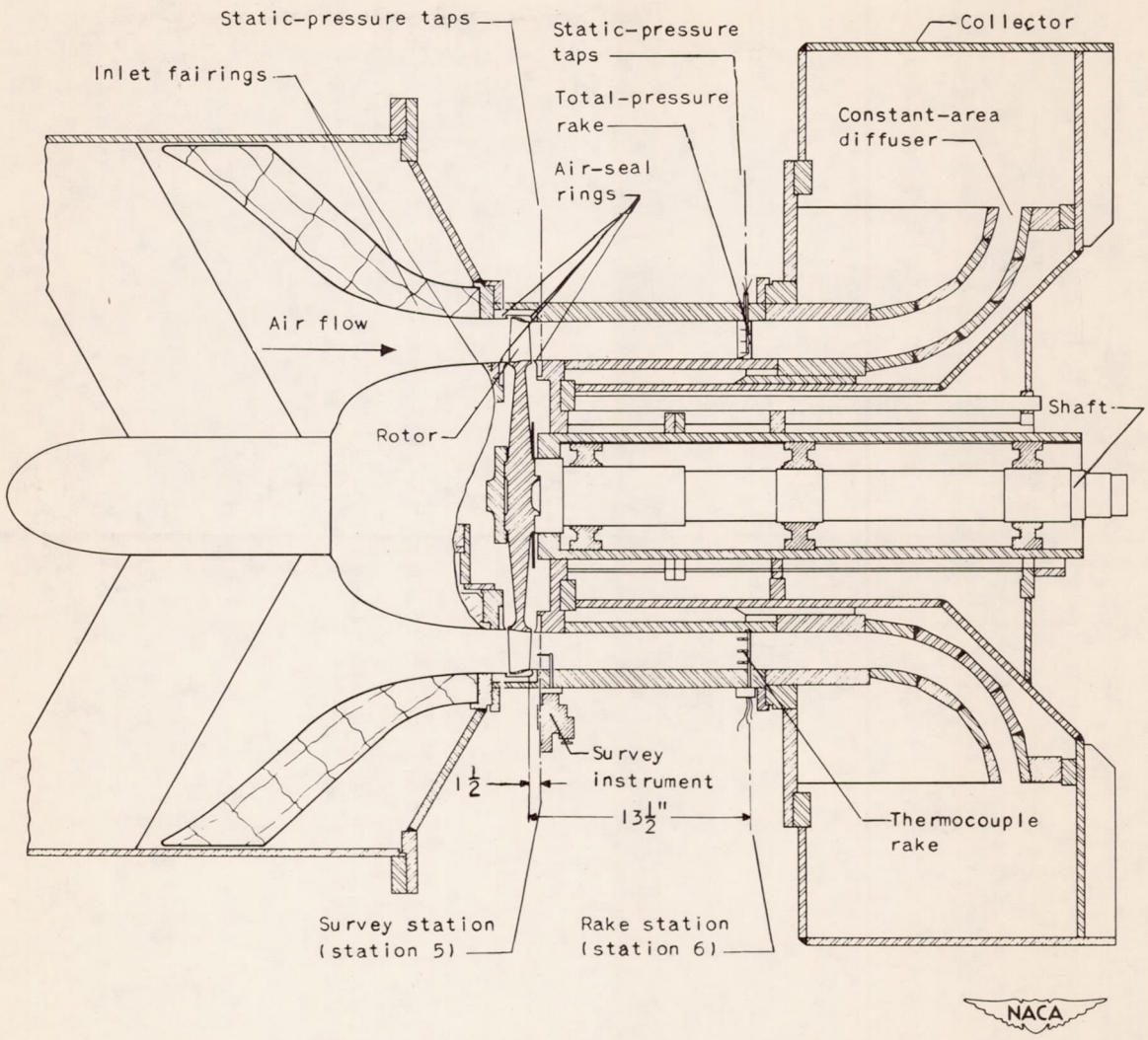

Figure 4. – Sectional view of variable-component supersonic-compressor installation.

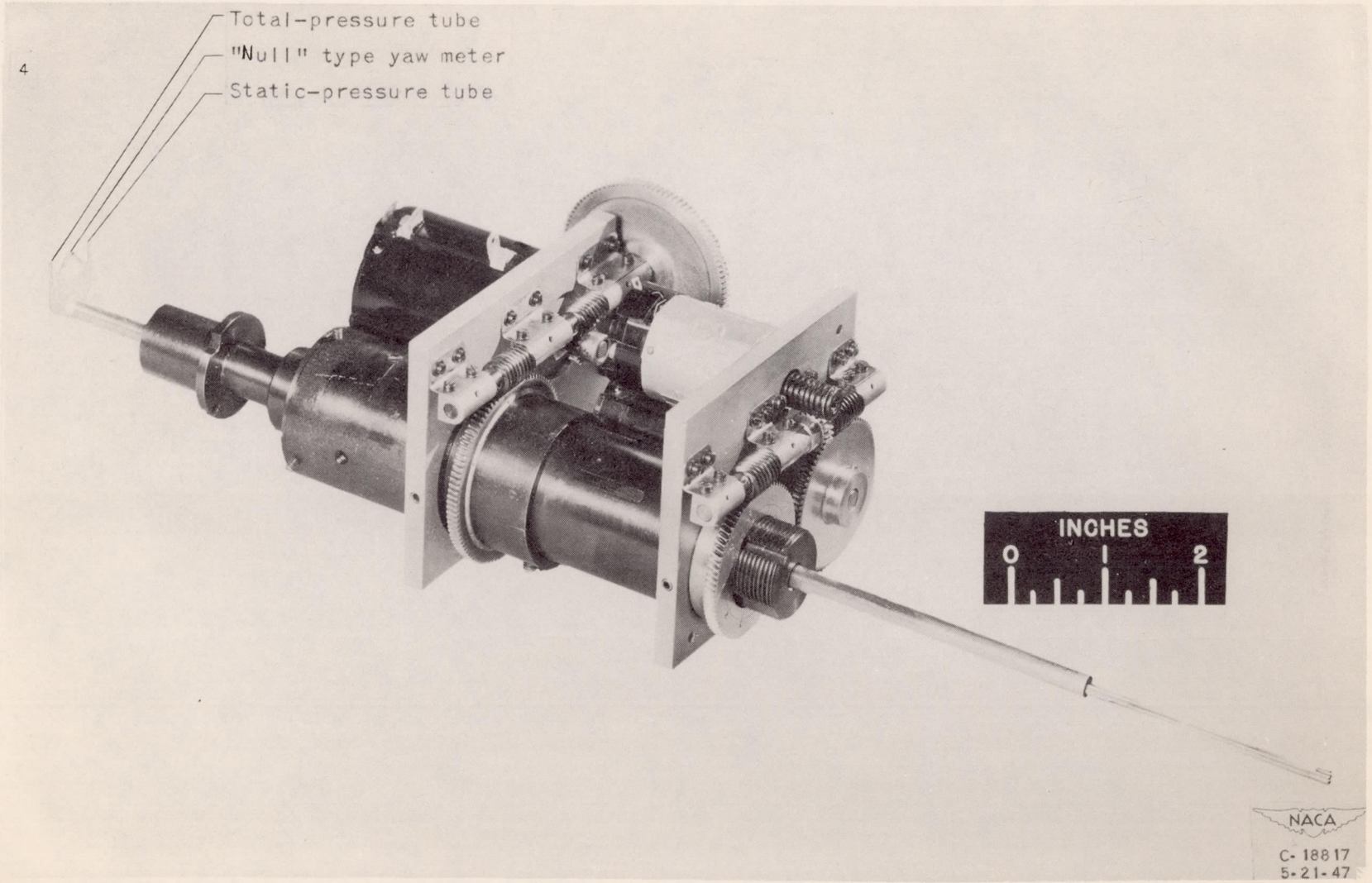

Figure 5. - Motor-driven survey instrument.

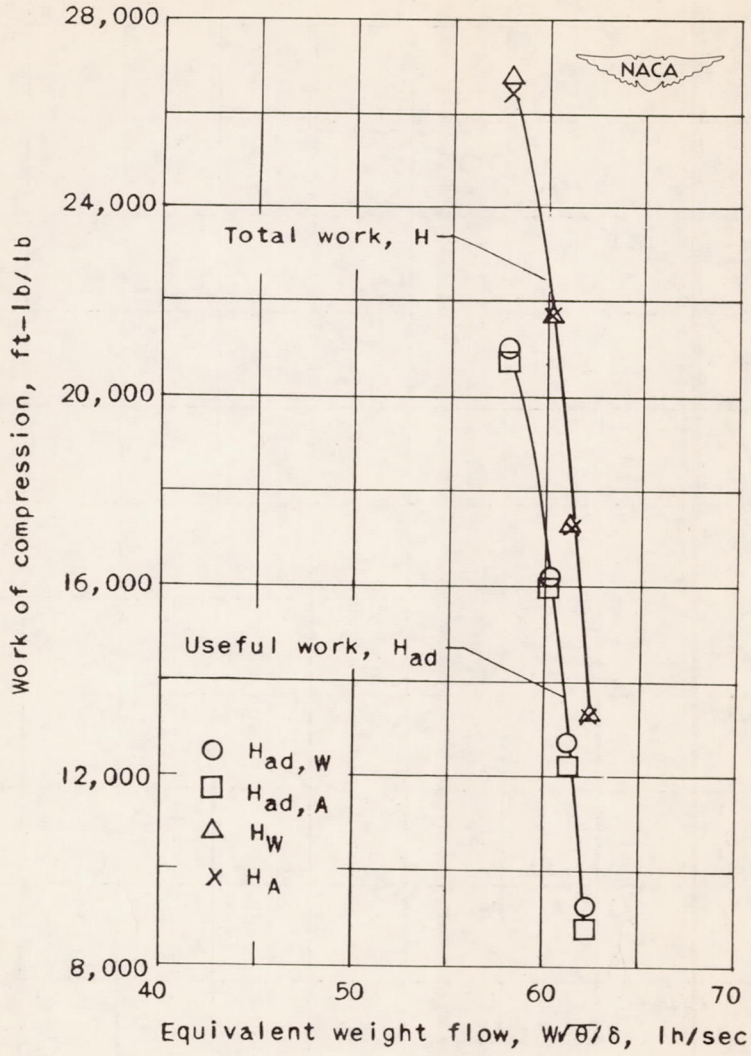

Figure 6. - Work of compression for 24-inch supersonic-compressor rotor at equivalent tip speed of 1608 feet per second.

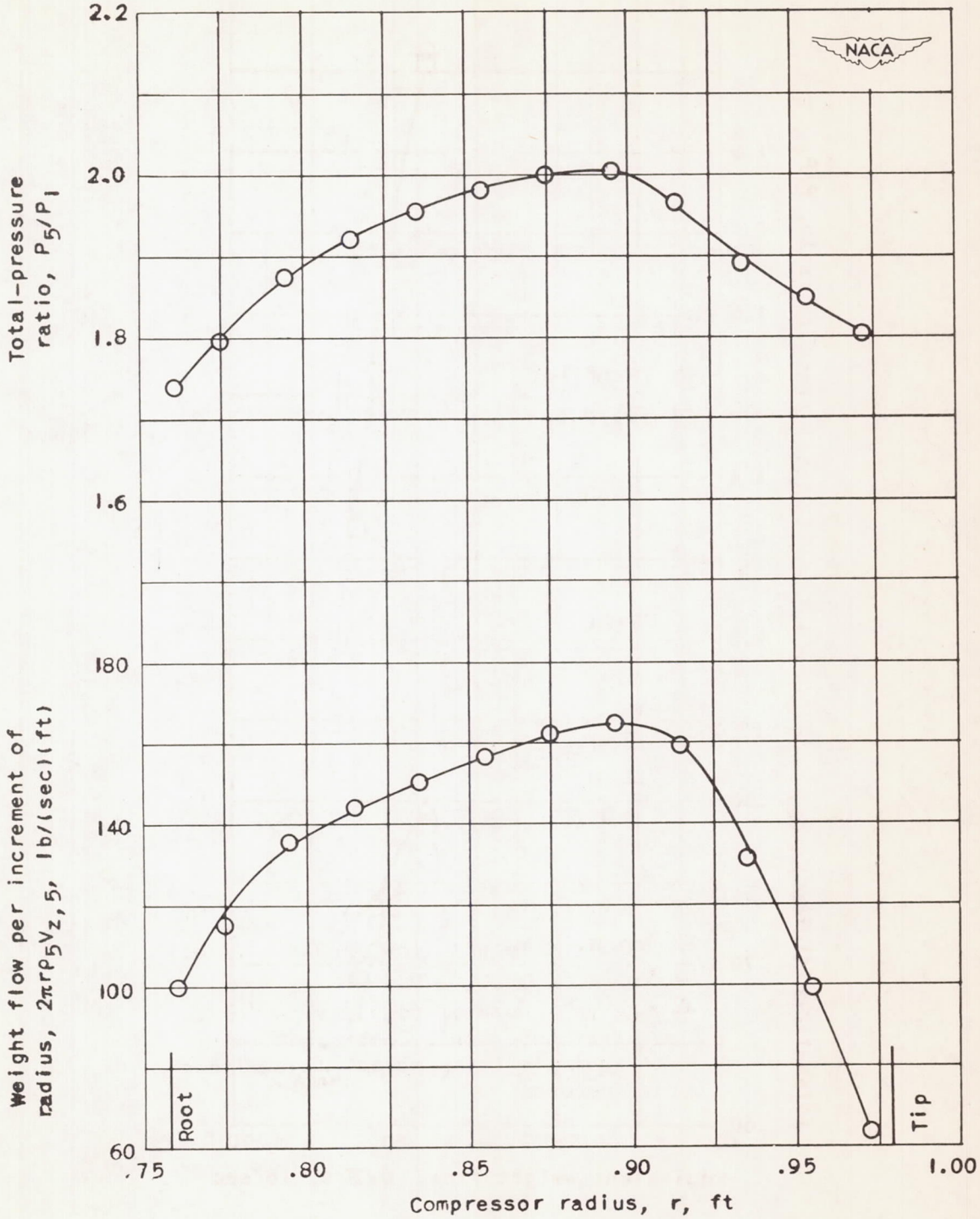

Figure 7. - Total-pressure-ratio and weight-flow profiles of 24-inch supersonic-compressor rotor measured at survey station. Equivalent tip speed, 1608 feet per second.

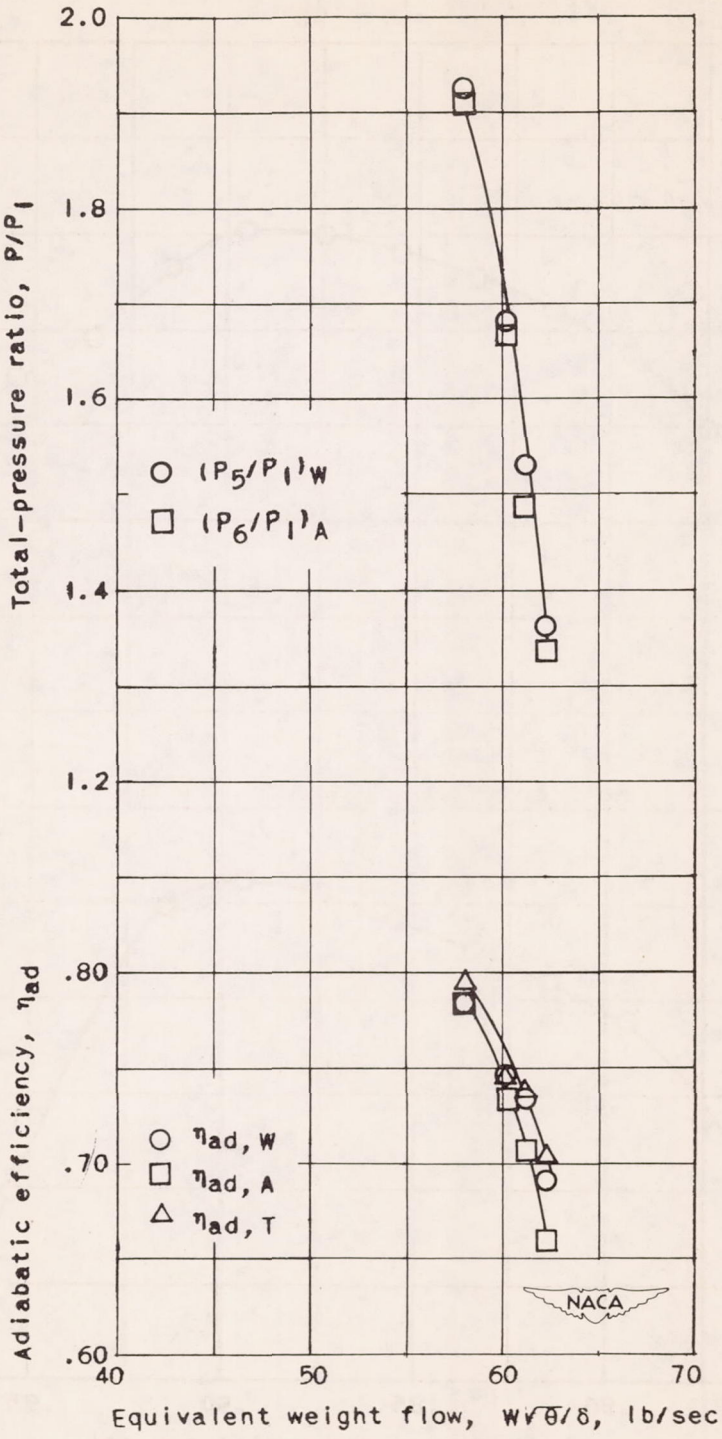

Figure 8. – Pressure ratio and adiabatic efficiency of 24-inch supersonic compressor rotor at equivalent tip speed of 1608 feet per second.